

## Modeling and Analysis of the Effect of Holes in Reinforced Concrete Column Structures

Yohanes Laka Suku\*, Kristoforus Je

Department of Civil Engineering, Universitas Flores, Ende, INDONESIA

\*Corresponding authors: [yohannessuku@gmail.com](mailto:yohannessuku@gmail.com)

**SUBMITTED** 13 August 2019 **REVISED** 5 September 2019 **ACCEPTED** 27 November 2019

**ABSTRACT** Holes are often made inside the column structure for plumbing, mechanical, and electrical installation purposes may affect the structural performance of the column. Therefore, this paper aims to model and analyze the effect of holes in reinforced concrete column structures due to lateral loads. Data were obtained from the reference frame structure of the previous researcher, with varying centric column holes of 0%, 2%, 4%, 6%, 8%, 10%, and 12%, respectively to the column cross-sectional area. Furthermore, a hole with a ratio of 4% to the column cross-sectional area was placed at 5 and 10 mm eccentric to the center of column cross-section to examine the influence of holes position in the perforated column. The frame structure was modelled and analyzed by Finite Element (FE) using ABAQUS software. The result showed that the maximum load, displacement, and crack pattern resulted from the model is close to the experimental result. The results of the analysis showed that with the hole size of 2% to 12% of the column cross-sectional area, the frame strength was reduced by 5.43% to 15.56%. The frame strength was also reduced by 2.77% and 6.14% when the hole placed 5mm and 10 mm eccentric to the center of the column cross-section area. The displacement of the frame also decreases by 59.63% to 74.60% when the holes with the ratio of 2% to 12% to the column cross-sectional area exist in the column. The existence of eccentric holes on the column reduced the performance of the frame structure, by decreasing its strength, displacement and ductility.

**KEYWORDS** Modelling and Analysis; Holes; Column; Concrete Structure

© The Author(s) 2020. This article is distributed under a Creative Commons Attribution-ShareAlike 4.0 International license.

### 1 INTRODUCTION

The reinforced concrete is a building material with relatively higher stiffness, resistant to fire, and possess lower construction costs. In the reinforced concrete building, pipes are often made *conduit* or holes are in the beam and column structure for plumbing, mechanical, and electrical installations. In column structure elements, the existence of a hole causes a reduction in cross-sectional area, and this certainly affects its mechanical properties.

The study of the effect of holes on column elements has been previously conducted. The result showed that the greater the hole size, the higher the axial load, flexural and column ductility, with less strength, and stiffness (Hoshikuma & Priestley (2000), Kim (2012), Ranzo & Priestley (2000), Zacoeb (2006)). Therefore, it is necessary to limit the size of holes in the column to ensure the structure's safety. In

contrast, the use of hollow column elements in the building can reduce its total weight, prevent earthquake loads, and produce an economic foundation size (Abhay (2014), Gaikwad & Kannan (2017)).

The effect of hollow columns on buildings needs to be assessed adequately because the response of hollow column structures due to earthquake loads may differ significantly. This study, therefore, aims to examine the behaviour of the hollow column frame structure related to its lateral force and the displacement relationship, its stiffness, and its ductility by varying the size and position of the hole in the column. In this study, the frame structure of the experimental results conducted by Mehrabi et al. (1994) was modelled and analyzed by Finite Element (FE) using ABAQUS software.

**2 RESEARCH METHOD**

The stages of the study started by modelling and analyzing the behaviour of reinforced concrete frames and steel reinforcement based on experimental research data conducted by Mehrabi et al. (1994). This was followed by defining the relationship between the stress and strain to the inelastic conditions of the damaged parameters. The input values of the model calibration result, namely the lateral force and displacement, are used as a reference to this study. The magnitude of the displacement measured is the average displacement at the end of the beam. Furthermore, a study of the behaviour of the frame structure was carried out by varying the size and position of the holes (eccentricity) towards the column center.

**3 FRAME STRUCTURE MODELLING**

The size of the frame structure used for modelling is shown in Figure 1, while the concrete and steel material quality data are presented in Table 1. The frame is constructed with vertical load ( $F_v$ ) on both columns of 66 kips (294 kN) and monotonic lateral loads ( $F_H$ ) on one end of the beam whose magnitude is gradually increased till it collapses.

The variations in holes size and position in the column are presented in Table 2 and Figure 2.

The modelling of frame structures is in accordance with geometric data as shown in Figure 1. The concrete column and beams element were modelled using an element of solid hexahedral which in ABAQUS is defined as a C3D8R element (Continuum 3D, linear 8-node brick, reduced integration). This element is used to reduce iterations during nonlinear analysis. Steel reinforcement is modelled using an element truss in the ABAQUS program defined as a T3D2 element (2-node linear 3-D truss), due to its ability to resist loads in the direction along its axis and produce values equivalent to the results of the analysis using solid elements (Birtel & Mark (2006), Cohen (2018), Genikomsou (2015), Genikomsou & Polak (2016), Grassl & Jirásek (2006), Nguyen & Korsunsky (2008)). The interaction between reinforcement and concrete is assumed to be perfectly attached. Therefore, an embedded region constraint was used to model the interactions between reinforcement and concrete elements to make them work as a single unit. Frame structure modelling is shown in Figure 3.

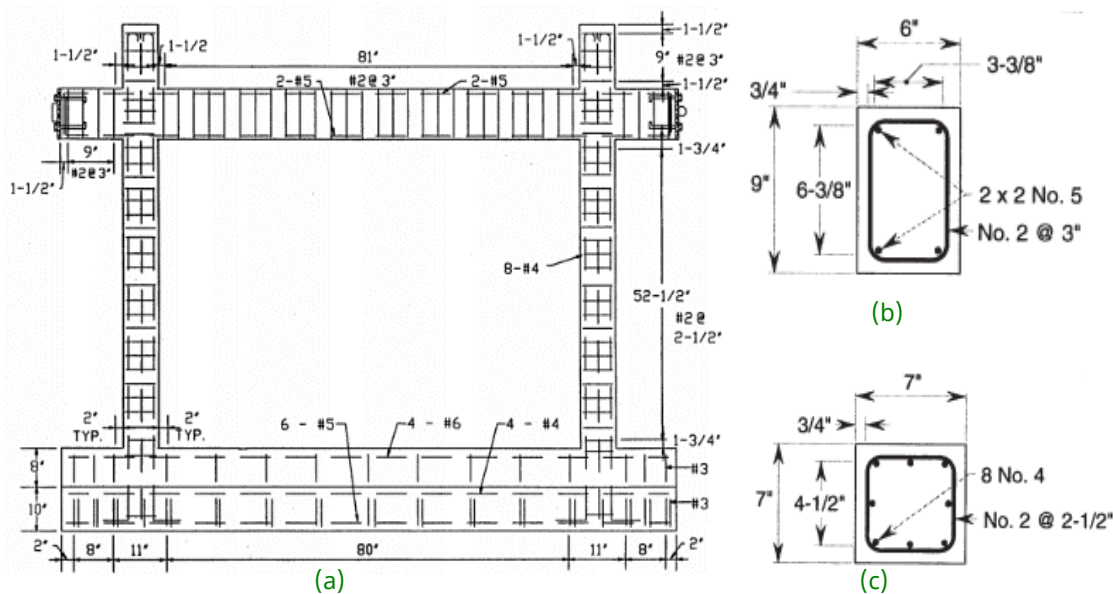


Figure 1. Reinforced concrete frame structure a) geometry; b) typical beam, c) typical column (Mehrabi et al, 1994)

Table 1. Quality of concrete and steel

<b>Concrete</b>				
Compression strength, ksi (MPa)	Tensile strength, $f_{ct}$ , ksi (MPa)	Strain at max compression strength, $\epsilon_{cu}$	Secant modulus, ksi (MPa)	
4.48 (30.889)	0.477 (3.289)	0.0018	3.180 (2,1925.334)	
<b>Steel</b>				
No	Diameter, inch (mm)	Yield strength, ksi (MPa)	Ultimate strength, ksi (MPa)	Modulus of elasticity, MPa
2	0.25 (6.35)	53.3 (367.49)	65.2 (449.54)	200,000
4	0.50 (12.70)	61.0 (420.58)	96.0 (661.90)	200,000
5	0.63 (15.88)	60.0 (413.69)	96.0 (661.90)	200,000

Table 2. Size and position of holes in columns

Ratio (%)	Diameter (mm)	$E_{cc}$ to column center (mm)	Description
0	0	0	Massive
2	28.5	0	Holes
4	40	0	Holes
4	40	5	direction x
4	40	10	direction x
6	50	0	Holes
8	57	0	Holes
10	64	0	Holes
12	70	0	Holes

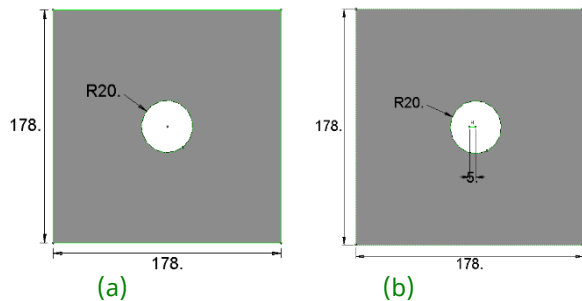


Figure 2. Cross-section of a hollow column diameter 40mm: a) center,  $E_{cc} = 0$ ; b)  $E_{cc} = 5$ mm

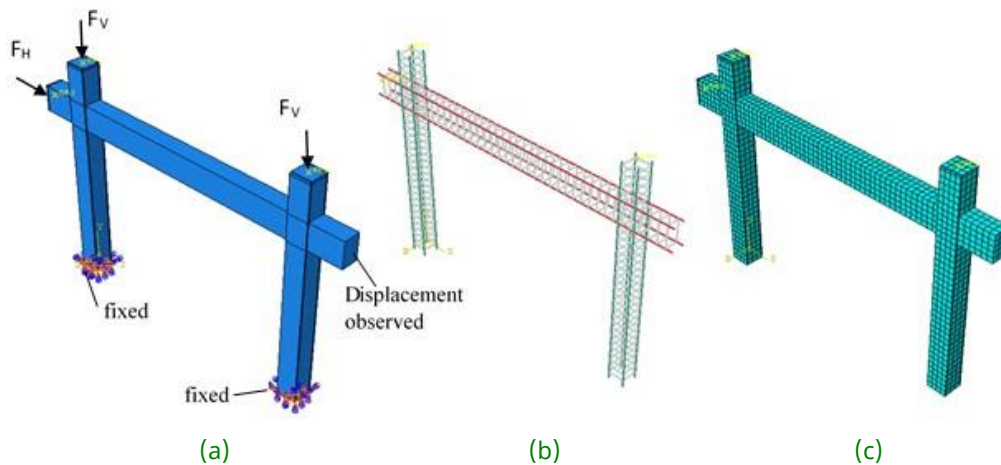


Figure 3. Model of reinforced concrete frame structures: a) solid element; b) reinforcement element; c) meshing of structure

#### 4 MATERIAL MODELING

The behaviour of concrete material and steel reinforcement is defined based on property data through empirical equations. The graph equation of stress and strain of compression concrete as proposed by Hognestad (1951) was used. This equation is often used as a reference in modelling concrete material behaviour with the ABAQUS program. The compressive stress-strain graph was modelled with parabolic relationships, as shown in Figure 4. The ascending and descending branches were calculated using Equation (1) and (2) as follows: The turning point of the calculated as the product of the constant  $k$ , which is equal to 0.9, with compression stress from the concrete cylinder test,  $f_c'$  ( $f_c' = 0.9 f_c''$ ) where  $f_c''$  is the peak stress, and  $\varepsilon_{co}$ , the strain. This constant is identified as the ratio between the compressions obtained from testing concrete cylinders with the actual strength (Hognestad, 1951). The graph is divided into three phases. The first phase is the linear-elastic phase when the first crack occurs in the stress range of  $0.4 f_c''$ . The second phase occurred when the maximum stress  $f_c''$  reached with strain  $\varepsilon_{co} = 2f_c''/E_0$ . The third phase occurred when the stress starts to decrease linearly with an increase in strain till its maximum value is reached  $\varepsilon_{cu}$ , and the magnitude of stress is assumed to be equal to 85%.

$$f_c = f_c'' \left[ \frac{2\varepsilon_c}{\varepsilon_{co}} - \left( \frac{\varepsilon_c}{\varepsilon_{co}} \right)^2 \right] \quad (1)$$

$$f_c = f_c'' \left[ 1 - 0,15 \left( \frac{\varepsilon_c - \varepsilon_{co}}{\varepsilon_{cmax} - \varepsilon_{co}} \right) \right] \quad (2)$$

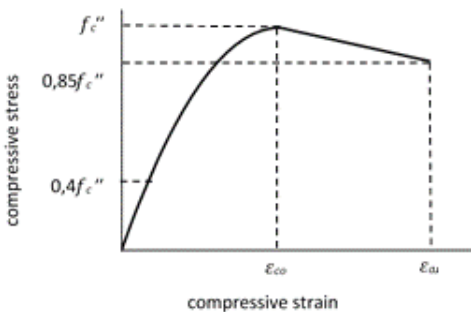


Figure 4. Compression concrete stress and strain graphs (Hognestad et al. 1955)

The concrete stress and strain equation in tension were approximated by the equation proposed by Belarbi & Hsu (1994). This is seen in Equation (3)

and (4), which are defined as functions of uniaxial tensile strain and uniaxial tensile stress. The tensile stress  $f_{ct}$  increases linearly to the peak value with  $\varepsilon_t = \varepsilon_{cr} = f_{ct}/E_c$ , then it decreases till the strain  $\varepsilon_t$ , is obtained, as shown in Figure 5.

$$f_t = E_c \cdot \varepsilon_t \text{ for } \varepsilon_t < \varepsilon_{cr} \quad (3)$$

$$f_t = f_{ct} \left( \frac{\varepsilon_{cr}}{\varepsilon_t} \right)^{0,4} \text{ for } \varepsilon_t > \varepsilon_{cr} \quad (4)$$

Furthermore, it determined the relationship of compression strain stress and tensile in inelastic conditions with the appropriate concrete damage plasticity. CDP is one of the constitutive models used to define the complex behaviour of concrete material during degradation, pressures and pulls (Genikomsou & Polak (2016), Grassl & Jirásek (2006), Hafezolghorani et al. (2017), Labibzadeh et al. (2017)). CDP parameters in the ABAQUS program consist of damage and plasticity parameters. The principle of damage parameter is explained based on concrete behaviour graphs for loading under inelastic conditions as shown in figure 6 (ABAQUS (2014), Birtel & Mark (2006), Cohen (2018), Genikomsou (2015)).

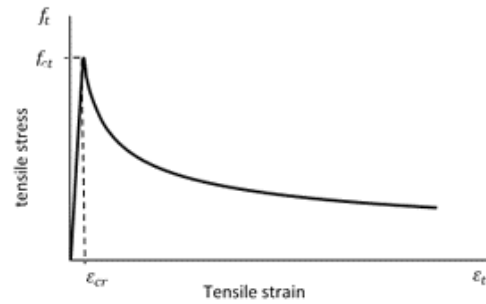


Figure 5. Concrete tensile stress and strain graphs (Belarbi & Hsu, 1994)

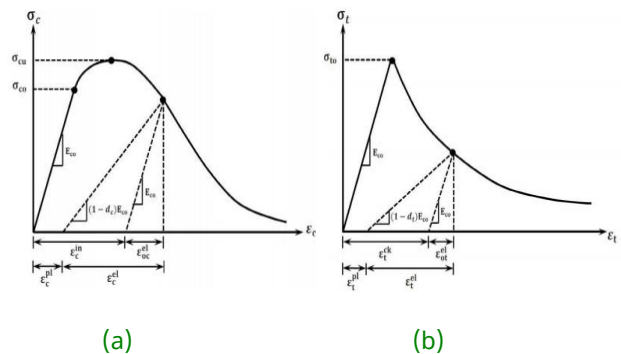


Figure 6. Concrete damage parameters: a) in compression; b) in tension

Based on figure 6 the magnitude of the concrete strain, which is compressed under destroyed conditions ( $\varepsilon_c^{in}$ ) and when cracked ( $\varepsilon_t^{ck}$ ), is calculated using the Equation (5) to (8).

$$\varepsilon_c^{in} = \varepsilon_c - \varepsilon_{oc}^{el} = \varepsilon_c - \frac{\sigma_c}{E_{co}} \quad (5)$$

$$\varepsilon_c^{el} = \varepsilon_c - \varepsilon_c^{pl} = \varepsilon_c - b_c \varepsilon_c^{in} \quad (6)$$

$$\varepsilon_t^{ck} = \varepsilon_t - \varepsilon_t^{el} = \varepsilon_t - \frac{\sigma_t}{E_{co}} \quad (7)$$

$$\varepsilon_t^{el} = \varepsilon_t - \varepsilon_t^{pl} = \varepsilon_t - b_t \varepsilon_t^{in} \quad (8)$$

Using a constant factor  $b_c$  and  $b_t$  with  $0 < b_c$  and  $b_t \leq 1$ . The parameter of concrete damage due to compressive stress ( $d_c$ ) and tensile stress ( $d_t$ ) is a function of the compressive plastic strain. The values of  $d_c$  and  $d_t$  range from 0 (concrete is undamaged) to 1 (broken/damaged concrete), are calculated using Equation (9) and (10).

$$d_c = 1 - \frac{\sigma_c}{E_{co}(\varepsilon_c - \varepsilon_c^{pl})} \quad (9)$$

$$d_t = 1 - \frac{\sigma_t}{E_{co}(\varepsilon_t - \varepsilon_t^{pl})} \quad (10)$$

The results of the analysis of the relationship between the stress-strain compression, concrete tensile strength and the parameters of damage to the inelastic condition are shown in Figures 7 and 8.

In addition to the damaged parameter, the plasticity is also important and needs to be defined in the CDP model. Five plasticity parameters need to be inputted on the ABAQUS software, that is the ratio of biaxial/uniaxial compressive strength ( $\sigma_{bo}/\sigma_{co}$ ), flow potential eccentricity ( $\varepsilon$ ), deviatoric stress invariant ratio ( $K_c$ ), viscosity parameter ( $\mu$ ), and dilation angle ( $\psi$ ). Parameters  $\mu$  and  $\psi$  have a certain value according to the characteristics of the concrete used, and its adjustment or calibration is essential (Birtel and Mark (2006), Cohen (2018), Genikomsou (2015), Genikomsou and Polak (2016), Hafezolghorani et al. (2017), Labibzadeh et al. (2017)). Meanwhile, the other parameters, values were adjusted by ABAQUS. The corresponding plasticity parameter values are shown in Table 3.

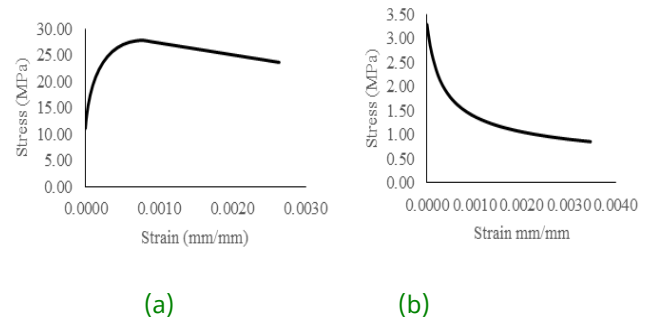


Figure 7. Graph of concrete stress and strain relationships in inelastic conditions: a) compressive, b) tensile

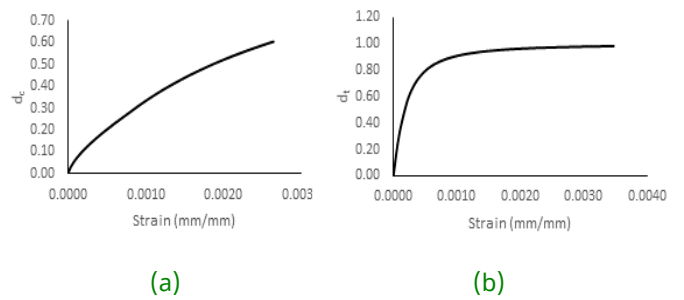


Figure 8. Graph of the relationship of concrete damage and strain parameters in inelastic conditions: a) compressive, b) tensile

Table 3. CDP model parameters

$\sigma_{bo}/\sigma_{co}$	$\varepsilon$	$K_c$	$\mu$	$\psi$
0.667	0.1	1.16	0.0001	40°

The relationship between stress and strain of steel reinforcement used the bilinear model, in which the value post modulus of elasticity ( $E_{sy}$ ) is taken as 1% of the modulus of elasticity ( $E_s$ ). The example of the relationship between stress and strain of steel reinforcement is shown in Figure 9.

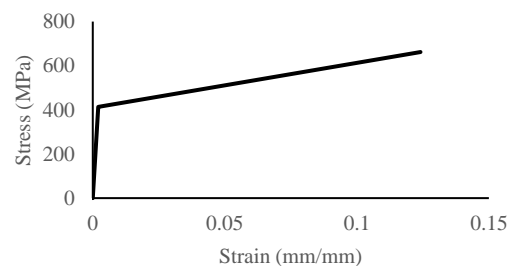


Figure 9. Graph relations of stress and strain for steel reinforcement No. 5

**5 RESULTS AND DISCUSSION**

**5.1. Verification Frame benchmark**

The FE analysis results of the reinforced concrete frame, in term of lateral load ( $F$ ) and displacement ( $D$ ), is close to experimental result with the difference of less than 1% as shown in Table 4. Furthermore, the load and displacement relationship have the same pattern as shown in Figure 10. Similarly, the crack that occurs in the frame as a result of the analysis of FE with the ABAQUS program has the same pattern as shown in Figure 11. Crack due to bending occurs at the column and beam, the crack due to shear occurs at the beam-to-column joint, thereby, causing failure on the frame. The results of this analysis indicate that the input data and the use of the ABAQUS software to model the frame structure are appropriate.

Table 11. Comparison of experimental results and ABAQUS

	Experimental	ABAQUS	Difference
$F_H$ (kN)	106.312	106.645	0.31%
$D$ (mm)	65.278	65.900	0.95%

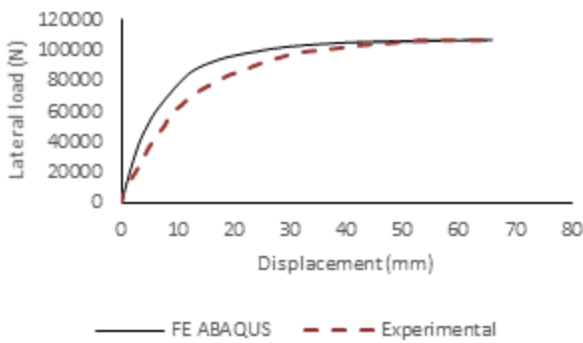


Figure 10. load-displacement curve comparison between experimental results and ABAQUS

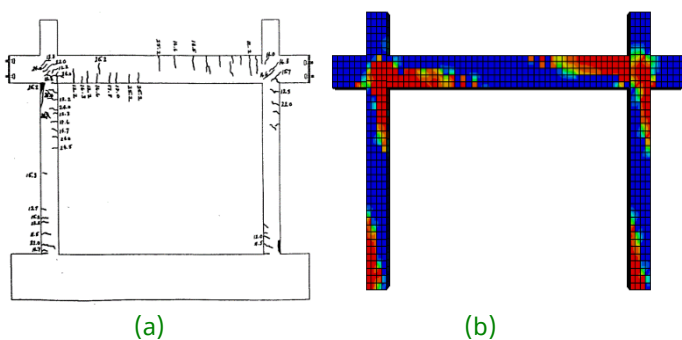


Figure 11. Crack pattern of the frame structure resulted from: a) experimental; b) ABAQUS

**5.2. Frame with Hole Column**

**5.2.1. Relationship between load and displacement**

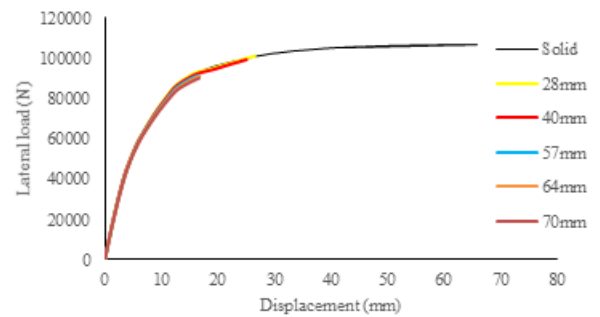
The results of load analysis and lateral displacement of the frame with hole columns are shown in Table 5, Table 6, and Figure 12.

Table 5. Lateral load ( $F_H$ ) and displacement ( $D$ ) frame with a hollow column

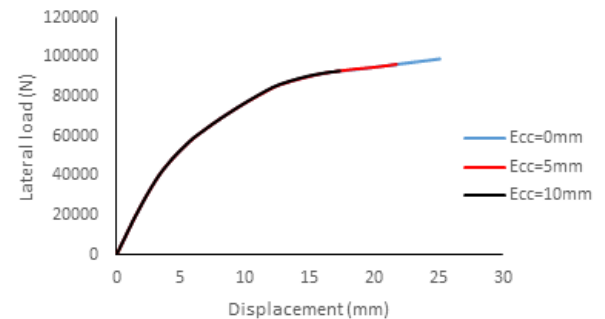
Ratio (%)	$F_H$ (kN)	$D$ (mm)	Difference (%)	
			$F_H$	$D$
0	106.645	65.900	0	0
2	100.854	26.607	-5.43	-59.63
4	99.182	25.088	-7.00	-61.93
6	92.199	16.648	-13.55	-74.74
8	91.423	16.561	-14.27	-74.87
10	91.023	16.789	-14.65	-74.53
12	90.051	16.739	-15.56	-74.60

Table 6. Load ( $F_H$ ) and displacement ( $D$ ) frames with perforated columns that are not centric

Ratio (%)	$E_{cc}$ (mm)	$F_H$ (kN)	$D$ (mm)	Difference (%)	
				$F_H$	$D$
4	0	99.182	25.088	0	0
4	5	96.438	21.712	-2.77	-13.46
4	10	93.092	17.314	-6.14	-30.99



(a)



(b)

Figure 12. Load-displacement curve of the frame with hollow columns: a) holes variations; b) eccentricity variations

The results of the analysis showed that the existence and eccentricity of holes in the columns reduced strength and displacement frame. In the hole size of 2% and 4% of the column cross-sectional area, the frame strength was reduced by 5.43% and 7.00%. Meanwhile, in the hole size of 6% to 12% of the column cross-sectional area, the frame strength was reduced by 13.55% to 15.56%. Indonesian National Standard concerning Requirements for Structural Concrete for Buildings Instruction (BSN, 2013) in article 6.3.4 limits the size of holes in the column to less than 4% of cross-sectional area, and article 6.3.5 states that a hole size larger than 4% is usable assuming it has been approved by a licensed professional designer. From the results of this analysis, it was found that in the 4%-hole size there was a reduction in frame strength by 7% and in 6% it reduced to 13.55%. This means that when the hole size is greater than 4%, it reduces strength frame by more than 10%.

Based on Figure 12, there was a significant displacement reduction caused by the frame that becomes more brittle due to the presence of holes in the column. When the hole size is 2%, it causes a reduction in the displacement of 59.63%; meanwhile at a 12% holes size, it causes a reduction in the displacement of 74.60%. The decrease in strength and displacement also occurred when the hole placed eccentric to the column cross-section, as shown in Table 6 and Figure 12.b. Therefore, in a 10 mm eccentricity, there is a reduction in strength and displacement by 6.14% and 30.99%, respectively.

### 5.2.2. Ductility and Stiffness

Ductility is defined as the ability of a structure to experience post-elastic deflection. It is also an important parameter in disseminating earthquake resistant structures. Ductility is needed for the structure to absorb the energy produced from inelastic deformations when an earthquake occurs without failure. Its need is inversely proportional to stiffness, where the higher the ductility characteristic of a structure, the smaller the stiffness. The ductility value ( $\mu$ ) is generally determined based on the ratio between the maximum displacement ( $\delta u$ ) and the first

yield time ( $\delta y$ ). While the structural rigidity ( $K$ ) is defined as the ability of the structure to deform under the influence of the load, with the magnitude of force determined based on the ratio between the maximum load ( $P_{max}$ ) and deflection ( $\delta u$ ). The structure's displacement during the first yield ( $\delta y$ ) is determined based on the idealized graph of load and displacement, where the ultimate load is not less than 80% of the maximum,  $P_{max}$  (Meharbi & Shing, 2003), as shown in Figure 13.

Based on Figure 13, the ultimate displacement is determined based on the maximum and lateral load-displacement ( $\delta m / \delta u$ ) of 80%. Displacement at yield ( $\delta y$ ) is obtained by determining the intersection point between the elastic stiffness lines ( $K_e$ ) to  $0.8P_{max}$ . The stiffness and ductility of the structure at the maximum displacement are seen in Table 7. Based on Table 7, it can be seen that existence of holes both in centric and eccentric position caused a decrease in ductility of the structure, thereby, making the frame more rigid.

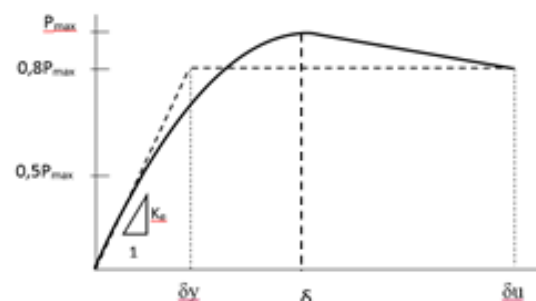


Figure 13. Graph of idealization of load and displacement relations

Table 7. Rigidity and ductility of frames with hollow columns

Ratio (%)	Stiffness (kN/mm)		Ductility
	$K_e$	$K$	$\mu$
0	10.474	1.618	8.014
2	10.962	3.791	3.615
4	11.194	3.953	3.540
4 ( $E_{cc}=5\text{mm}$ )	11.213	4.441	3.156
4 ( $E_{cc}=10\text{mm}$ )	11.578	5.376	2.692
6	11.355	5.538	2.563
8	11.371	5.520	2.573
10	11.378	5.421	2.623
12	11.399	5.379	2.648

## 6 CONCLUSIONS

As conclusion, frame structure modeling and analysis using ABAQUS software showed that the predicted results of the load-displacement curve and crack patterns that occurred were close to the experimental results. Furthermore, the existence and the eccentricity of holes in the columns led to a decrease in the performance of frame structure, which decreases in strength, displacement, and ductility, thereby, making the frame structure more rigid and brittle. At the 4%-hole ratio which is the maximum size permitted by the Indonesian National Standard on Structural Concrete Requirements for Buildings, there is a reduction in the strength of frame structure by 7%, 61.93% displacement, and ductility of 44.17%, while the stiffness increases by 244%.

## DISCLAIMER

The authors declare no conflict of interest

## REFERENCES

ABAQUS, 2014. *Abaqus Analysis User's Guide*. USA: Dassault Systèmes Simulia.

Abhay, 2014. Comparison of Seismic Performance of Solid and Hollow Reinforced Concrete members in RCC framed Building using ETABS Software. *International Journal of Advances in Engineering Sciences* 4(4), pp. 43-47.

Belarbi, A. & Hsu, T.T.C., 1994. Constitutive Laws of Concrete in Tension and Reinforcing Bars Stiffened by Concrete. *ACI Structural Journal* 91(4), pp. 465-474.

Birtel, V. & Mark, P., 2006. Parameterised Finite Element Modelling of RC Beam Shear Failure *ABAQUS Users' Conference*. Boston, Mass, ABAQUS, Inc. 95-108.

BSN, 2013. *Persyaratan Beton Struktural untuk Bangunan Gedung (SNI 2847: 2013)* Jakarta: Badan Standardisasi Indonesia (BSN).

Cohen, M., 2018. Numerical Analysis of Debonding Mechanisms of Externally Bonded FRP Reinforcement in RC Beams. *Civil Engineering*. Waterloo, Ontario, Canada, University of Waterloo.

Gaikwad, S.A. & Kannan, R., 2017. Analysis and Design of Hollow Reinforced Concrete Columns. *International Journal on Recent and Innovation Trends in Computing and Communication* 5(4), pp. 138-142.

Genikomsou, A., 2015. Nonlinear Finite Element Analysis of Punching Shear of Reinforced Concrete SlabColumn Connections. *Civil Engineering*. Waterloo, Ontario, Canada, University of Waterloo.

Genikomsou, A. & Polak, M.A., 2016. Damaged plasticity modelling of concrete in finite element analysis of reinforced concrete slabs. *9th International Conference on Fracture Mechanics of Concrete and Concrete Structures*. University of California, Berkeley, California USA. 1-8.

Grassl, P. & Jirásek, M., 2006. Damage-plastic model for concrete failure. *International Journal of Solids and Structures* 43(22-23), pp. 7166-7196.

Hafezolghorani, M., Hejazi, F., Saleh, M. & Karimzade, K., 2017. Simplified Damage Plasticity Model for Concrete. *Structural Engineering International* 27(1), pp. 68-78.

Hognestad, E., 1951. *A study of combined bending and axial load in reinforced concrete*. University of Illinois at Urbana-Champaign.

Hognestad, E., Douglas, N.W.H. & McHenry, 1955. Concrete Stress Distribution in Ultimate Strength Design. *ACI Journal Proceedings* 52(12).

Hoshikuma, J.I. & Priestley, M.J.N., 2000. Flexural Behavior of Circular Hollow Columns with Single Layer of Reinforcement Under Seismic loading, Report No. SSRP-2000/13. University of California, San Diego, CA.

Kim, T.H., 2012. Inelastic Behavior of Hollow Reinforced Concrete Bridge Columns. *15th WCEE*.

Labibzadeh, M., Zakeri, M. & Adel Shoaib, A., 2017. A new method for CDP input parameter identification of the ABAQUS software guaranteeing uniqueness and precision. *International Journal of Structural Integrity* 8(2) 264-284.

Meharbi, A.B. & Shing, P.B., 2003. Seismic Analysis of Masonry-Infilled Reinforced Concrete Frames. *TMS Journal* 21(1), pp. 81-94.

Mehrabi, A.B., Shing, P.B., Schuller, M.P. & Noland, J.L., 1994. *Performance of Masonry-Infilled Reinforced Concrete Frame Under In-Plane Lateral Loads, Research Series No. CU /SR-94/6* Department of Civil, Environmental, & Architectural Engineering University of Colorado at Boulder, CO 80309-0428

Nguyen, G.D. & Korsunsky, A.M., 2008. Development of an approach to constitutive modelling of concrete: Isotropic damage coupled with plasticity. *International Journal of Solids and Structures* 45(20), pp. 5483-5501.

Ranzo, G. & Priestley, M.J.N., 2000. Seismic Performance of Large RC Circular Hollow Columns *12th WCEE*.

Zacoeb, A., 2006. Ductility of Hollow RC Short Columns in Compression Region. *Dinamika TEKNIK SIPIL* 6(1), pp. 1-6.

[This page is intentionally left blank]